

Particle Orbits and Radial Loss in the GAMMA10 Tandem Mirror

ITO Toru and KATANUMA Isao

Plasma Research Center, University of Tsukuba, Ibaraki 305-8577, Japan

(Received: 17 December 2003 / Accepted: 14 May 2004)

Abstract

Ion orbits trapped in the transition mirror cells with non-axisymmetric magnetic field in GAMMA10 are calculated. It is found that those orbits are deviated from the magnetic flux tube. The results indicate the existence of “radial loss cone” in view of the limiter. The radial drift due to the radial loss cone is examined numerically and analytically.

Keywords:

non-axisymmetric magnetic field, radial transport, tandem mirror, GAMMA10

1. Introduction

The experimental results in the GAMMA10 tandem mirror have demonstrated the improvement of the axial plasma confinement. So the radial loss can not be disregarded. There could be some reasons to cause it. We especially pay attention to the radial transport due to the non-axisymmetric magnetic field in this research. GAMMA10 is essentially designed as an axi-symmetrized tandem mirror. Particles passing through the mid-plane in the GAMMA10 central cell are expected not to drift for a radial direction. However GAMMA10 consists of not only central mirror cell but other mirror cells. Especially there are mirror cells called transition mirror cell, where the magnetic field is not axial symmetry. It has been reported that the particle trapped in the mirror cell could be caused large radial drift.[1]

We calculate the orbits in GAMMA10 magnetic field without electrostatic potential and investigate the feature of radial drift due to the non-axisymmetric magnetic field in the transition mirror cell precisely. Additionally, we examine the particle radial loss in the velocity space, and find “radial loss cone”.

2. Radial drift due to the non-axisymmetric magnetic field

To illustrate the feature of the particle orbits in the transition mirror cell with non-axisymmetric magnetic field in GAMMA10, we first consider the ions trapped in the transition mirror cell centered around $z = 367\text{cm}$, anchor mirror cell centered $z = 520\text{cm}$, another transition mirror cell centered $z = 673\text{cm}$ in Fig. 1 respectively.

We adopt the paraxial approximation to the magnetic field with the flux coordinates (ψ, θ, ζ) , the equations of motion are written as

$$\begin{aligned} \frac{d\psi}{dt} &= -\frac{c}{q} k_\theta (2\varepsilon - \mu B), \\ \frac{d\theta}{dt} &= \frac{c}{q} k_\psi (2\varepsilon - \mu B), \\ \frac{dz}{dt} &= v_\parallel, \\ \mathbf{B} &= \nabla\psi \times \nabla\theta, \quad \mathbf{k} = k_\psi \nabla\psi + k_\theta \nabla\theta, \\ \psi &= \frac{1}{2} r^2 B_0, \end{aligned} \quad (1)$$

where z is the coordinate along the mirror axis and $z = 0$ at the central mirror cell mid-plane \mathbf{B} is the magnetic field, $B_0 = B(z_c)$ is the magnetic amplitude at the central mirror cell mid-plane, c is the light velocity, $2\pi\psi$ is the magnetic flux, ε is the energy of particle, μ is the magnetic moment of particle, q is the electric charge, r is the radial distance in terms of the value at central mirror cell mid-plane. \mathbf{k} is the curvature of magnetic field line, where k_ψ and k_θ are the normal and geodesic curvatures with the following relations,

$$\begin{aligned} k_\psi &= \frac{1}{2} \hat{k}_\psi - \frac{1}{2} \hat{k}_\theta \cos 2\theta, \\ k_\theta &= \hat{k}_\theta \psi \sin 2\theta, \\ \hat{k}_\psi &= \frac{\sigma''\sigma + \tau''\tau}{B_0}, \\ \hat{k}_\theta &= -\frac{\sigma''\sigma + \tau''\tau}{B_0}, \\ x &= \sigma(z)x_0, \quad y = \tau(z)y_0, \end{aligned} \quad (2)$$

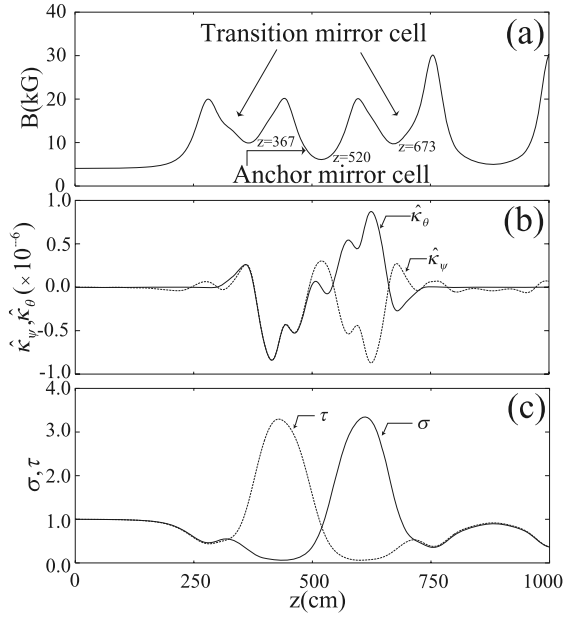


Fig. 1 Axial magnetic field profile in the GAMMA10 tandem mirror. (a) Magnitude of magnetic field. (b) Normal curvature \hat{k}_ψ and geodesic curvature \hat{k}_θ of magnetic field line. (c) σ and τ in eq. (2).

where θ is the azimuthal coordinate, (x, y) are the coordinate of the magnetic field line starting from (x_0, y_0) at the mid-plane in the transition mirror cell, the primes denote derivatives with respect to z .

We examine the Poincare plot at the mid-plane in the transition mirror cell in terms of solving eq. (1) to consider the ion orbits trapped in each mirror cell that is the transition mirror cell centered around $z = 367\text{cm}$ and $z = 673\text{cm}$.

We set ions on the magnetic flux tube at $z = 367\text{cm}$ and $z = 673\text{cm}$ corresponding to $r = 1\text{cm}$ at the mid-plane in the central mirror cell and get off with several azimuthal coordinates θ and pitch angles. Figure 2 shows the Poincare plot at the mid-plane in the transition mirror cell at $z = 367\text{cm}$ (a), (b), (c) and $z = 673\text{cm}$ (d), (e), (f). The ions trapped in this mirror cell drift radially and deviate from the magnetic flux tube significantly because the radial displacement piles up by those bounce motion in the non-axisymmetric magnetic field. Besides the orbits turn into hyperbolic or elliptic sensitively depending on the initial pitch angle. The ions with elliptic orbit rotate in the azimuthal direction sufficiently, the others with hyperbolic orbit do not rotate in the azimuthal direction. Consequently the ions continue to drift out radially in case of hyperbolic orbits.

Because it is found that the non-axisymmetric magnetic field causes the large radial drift, we examine the particle orbits precisely in the next place.

Integrating eq. (1) through the one bounce motion by using eq. (2), we obtain the amount of $\Delta\psi$ and $\Delta\theta$, where $\Delta\psi$ and $\Delta\theta$ are the displacement of radial coordinate ψ and azimuthal coordinate θ for one bounce time. Assuming the displacement of ψ and θ during the one bounce motion is small, $\Delta\psi$ and $\Delta\theta$ are described as

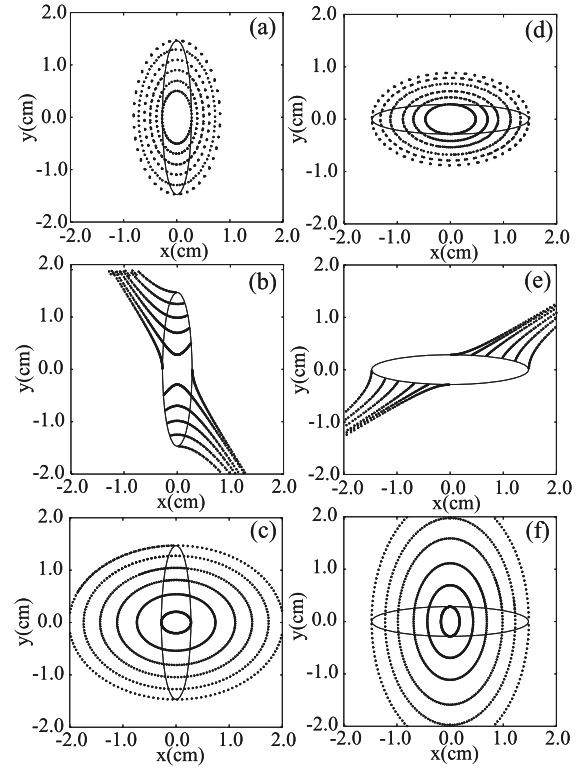


Fig. 2 Poincare plot at $z = 367\text{cm}$ plane (a), (b), (c) and $z = 673\text{cm}$ plane (d), (e), (f). The solid line is magnetic flux tube, and dots are ion orbits which given different initial pitch angle p_0 and started on the magnetic flux tube. (a)(d) $p_0 = 55$. (b)(e) $p_0 = 65$. (c)(f) $p_0 = 75$.

$$\begin{aligned}\Delta\psi &= c_1(\varepsilon, \mu) \psi \sin 2\theta, \\ \Delta\theta &= c_2(\varepsilon, \mu) + \frac{1}{2} c_1(\varepsilon, \mu) \cos 2\theta,\end{aligned}$$

$$\begin{aligned}c_1(\varepsilon, \mu) &= -\oint \frac{c}{q} (2\varepsilon - \mu B) \hat{k}_\theta \frac{dz}{v_\parallel}, \\ c_2(\varepsilon, \mu) &= \oint \frac{c}{2q} (2\varepsilon - \mu B) \hat{k}_\psi \frac{dz}{v_\parallel},\end{aligned}\quad (3)$$

the symbol \oint carries out the integration along one ion axial bounce in the mirror cell. Assuming that the ion drift velocity is much smaller than thermal velocity, the differential equation of $\psi(\theta)$ is described as

$$\frac{d\psi}{d\theta} = \frac{c_1(\varepsilon, \mu) \psi \sin 2\theta}{c_2(\varepsilon, \mu) + \frac{1}{2} c_1(\varepsilon, \mu) \cos 2\theta}.\quad (4)$$

The solution of eq. (4) is

$$\psi(\theta) = \frac{A}{c_2(\varepsilon, \mu) + \frac{1}{2} c_1(\varepsilon, \mu) \cos 2\theta},\quad (5)$$

where $A = \psi_0 \left[c_2(\varepsilon, \mu) + \frac{1}{2} c_1(\varepsilon, \mu) \cos 2\theta_0 \right]$, ψ_0 and θ_0 are initial value of ψ and θ . Figure 3 shows the comparison of ion orbits in terms of eq. (5) with the numerical calculation in

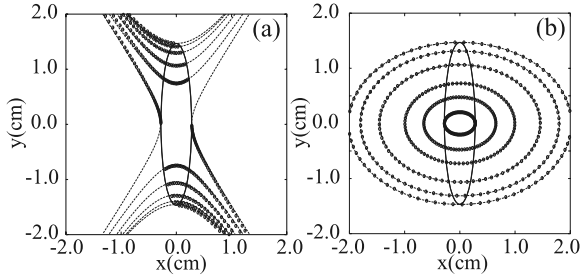


Fig. 3 Comparison of numerical calculation (circle) and analytical calculation (dashed line) by eq. (5) about ion orbits.

the case Figs. 2(b) and 2(c). The good agreement in Fig. 3 shows that the ion orbits are described by eq. (5). Additionally eq. (5) is similar to the description of quadratic curve in the polar coordinate. $c_1(\varepsilon, \mu)$ in eqs. (3) and (5) has a non-zero value in the non-axisymmetric transition mirror cells. Because the coefficient $c_1(\varepsilon, \mu)$ is a function of pitch angle, i.e., μ/ε , particle orbits has two types of elliptic and hyperbolic depending on the pitch angle of particles.

Because the radial drift of ion depends on the pitch angle, it is important to investigate the loss-cone region in the velocity space. We judge the ion radial loss by the radial distance r_w in terms of the value at the central mirror cell mid-plane. We set many ions with different energy and magnetic moment in the transition mirror cell centered around $z = 367\text{cm}$ and $z = 673\text{cm}$, pursuit the orbits. We see the ion that reaches a threshold r_w of radial distance as the loss ion, experimentally there are limiters corresponding to r_w with $r_w = 20 \sim 30\text{cm}$. Figure 4 shows the radial loss of ions in the velocity space, where (a) is the case of threshold $r_w = 20\text{cm}$, (b) is the case of $r_w = 30\text{cm}$, (c) is the case of $r_w = 40\text{cm}$, (d) is the case of $r_w = 100\text{cm}$.

Similar results are obtained about each transition mirror cell. The lost ions illustrated in Fig. 4(d) correspond to the ion drawing hyperbolic orbits. There are two radial loss

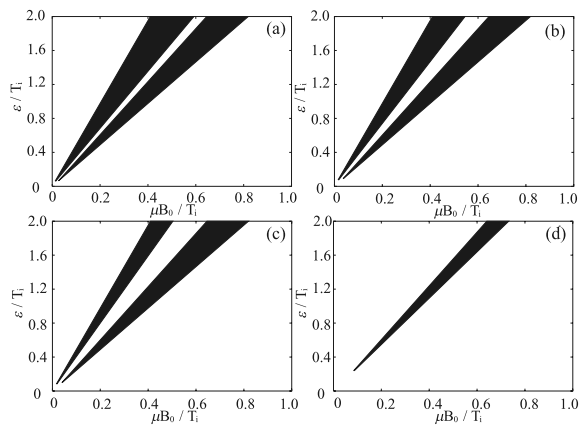


Fig. 4 Distribution of radial loss ions trapped in the transition mirror cells in the velocity space. (a) $r_w = 20\text{cm}$. (b) $r_w = 30\text{cm}$. (c) $r_w = 40\text{cm}$. (d) $r_w = 100\text{cm}$.

regions in the velocity space in Figs. 4(a)-(c), where ions in each region rotate in different azimuthal direction. We have calculated the ion orbits trapped in the transition mirror cells and found that some orbits deviate from the magnetic flux tube significantly. The existence of these orbits could affect the negative consequences on the plasma confinement. Finally we evaluate the orbital loss due to the radial drift in the non-axisymmetric transition mirror cells in GAMMA10.

We assume that the initial ions are Maxwellian,

$$f(\varepsilon) = \left(\frac{m_i}{2\pi T_i} \right)^{3/2} \exp\left(-\frac{\varepsilon}{T_i}\right), \quad (6)$$

the axial and azimuthal distribution is distributed uniformly, and the radial number density distribution is assumed as

$$n(\psi) = n_0 \exp\left(-\frac{\psi}{\psi_s}\right). \quad (7)$$

Here n_0 is the number density at ψ , and ψ_s is the coordinate at magnetic flux tube corresponds to $r = 20\text{cm}$ at the mid-plane in the central mirror cell. In these initial conditions, all ions have different orbits with each other. When an ion reached a threshold r_w , we count that the ion is lost radially. So ions are only lost radially, but are not lost axially. We change the threshold $r_w = 10\text{cm}, 20\text{cm}, 30\text{cm}, 100\text{cm}$ respectively. Figure 5 shows the axial density distribution of test ions after sufficient time compared with the azimuthal drift period has passed. The radial ion loss arises extremely only in the non-axisymmetric transition mirror cells, (the region of density dip in Fig. 5) hardly in the axisymmetric mirror cells. We note that the axial distribution in the transition mirror cells formed bumps. This corresponds to the radial loss particle in the velocity space are divided into two in Figs. 4 (a), (b), (c).

3. Summary and discussion

We especially take notice of the mirror cells called transition mirror cell in GAMMA10. The magnetic field is non-axisymmetric in the mirror cells. The ion orbits trapped in the mirror cell are calculated and as illustrated by Fig. 2 that the ions trapped in the transition mirror cells drift radially and deviate largely from the magnetic flux tube. It is confirmed that the radial drift is caused by the non-axisymmetric magnetic field.

We find that the ion orbits trapped in the non-axisymmetric magnetic field orbits turn into hyperbolic or elliptic by the pitch angle. The form of ion orbit depends on the pitch

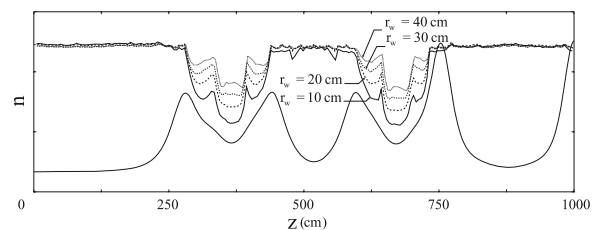


Fig. 5 Axial number density of ion in each magnetic flux tube.

angle.

These ions deviated largely from the magnetic flux tube could not be trapped radially. So we examine that what ion in the velocity space is not able to trap radially in the non-axisymmetric magnetic field transition mirror cells in GAMMA10. We find out the “radial loss cone” illustrated as Fig. 3. The ions in this region escape radially.

We neglected the electrostatic potential in this paper. If the radial electric field exists, some ions can escape from the loss-region due to the $\mathbf{E} \times \mathbf{B}$ drift. So the radial loss would be smaller.

We consider the radial drift velocity v_r of ion in the radial loss cone in terms of eq. (1), the radial loss time $\tau_{loss} = r_w / v_r$ is estimated as $\tau_{loss} \simeq \frac{r_w r q B_0 \int_{turn} dz}{c(2E - \mu B) \int_{turn} k \theta dz}$ by assuming that $\frac{d\theta}{dt} \sim 0$ in the radial loss cone. The loss cone angle due to the radial drift is about 10° in Fig. 4(b), so the collisional filling

time $\tau_{filling}$ is determined by the relation $\frac{\langle (10^\circ)^2 \rangle}{\tau_{filling}} \simeq \frac{\langle (90^\circ)^2 \rangle}{\tau_{collision}}$. In case of $T_i = 1\text{keV}$ and $n_i = 10^{12}\text{cm}^{-3}$, τ_{loss} and $\tau_{filling}$ are estimated as $\tau_{loss} \simeq 7\text{ms}$ and $\tau_{filling} \simeq 2\text{ms}$. $\tau_{filling} \ll \tau_{loss}$ is satisfied, so the assumption of Maxwellian distribution is valid.

References

- [1] Md. K. Islam, Y. Nakashima, K. Yatsu and I. Katanuma, *et al.*, J. Phys. Soc. Jpn. **69** (2000) 2493.
- [2] I. Katanuma, Y. Kiwamoto, M. Ichimura, T. Saito and S. Miyoshi, Phys. Fluids B. **5** (1990) 994.
- [3] J.A. Byers, Nucl. Fusion **22** (1982) 49.
- [4] R. Minai, I. Katanuma and T. Tamano J. Phys. Soc. Jpn **66** (1997) 2051.
- [5] R. Minai, I. Katanuma, T. Tamano and K. Yatsu, J. Phys. Soc. Jpn. **67** (1998) .